

# A Comparative Analysis on Application of PI and LQR Based Control for Speed Tracking of a DC Motor

Souvik Roy

Dept. of Applied Physics

University of Calcutta

Kolkata, West Bengal, India.

souvik\_roy1993@yahoo.co.in

Arijit Basak

Dept. of Applied Physics

University of Calcutta

Kolkata, West Bengal, India.

arijitbasak.basak@gmail.com

Abhishek Majumder

Dept. of Electrical Engg.

Future Institute of Technology

Kolkata, West Bengal, India.

abhishekmajumder2010@gmail.com

Sumana Chowdhuri

Dept. of Applied Physics.

University of Calcutta

Kolkata, West Bengal, India.

cu05sumana@gmail.com

**Abstract**— DC motors have found extensive industrial usage due to their wide range of speed control and excellent speed torque characteristics. The simplest speed control technique for dc motor is the proportional integral (PI) control due to its ease of implementation since all the control variables are dc quantities. Improved performance can be achieved by using other control techniques like deadbeat control, fuzzy logic control, model predictive control and state feedback control. The optimal control approach of state feedback is Linear Quadratic Regulator (LQR) control which has been proven to achieve better control action compared to classical control approaches. This paper emphasizes on the mathematical approach to design the LQR controller for speed control of a DC motor by converting the reference tracking problem into a regulator problem. The controller has been designed in the Simulink environment of MATLAB and the performance of the designed controller is compared to that of a PI based controller.

**Keywords**— dc motor, LQR, speed control, state feedback

## I. INTRODUCTION

DC motors are popular due to their wide range of speed control, high starting torque, high accelerating and decelerating torques. They are widely used in industry to cater high torque requirements and speed control applications. They are preferred over other types of motors due to their relatively easy drive circuits for speed control. Consequently, a variety of controllers and control topologies for the position and speed control of dc motors are available in the literature. For speed control up to rated speed, armature voltage control method is generally used where the voltage supplied to the motor armature is controlled. For speed control above rated speed, the motor field strength is controlled by controlling the motor field current [1].

The simplest controller in use is the proportional integral (PI) controller which reduces the error between the motor's actual speed and reference speed [2]. PI controller is easy to implement as the measured quantities are dc but it suffers from the drawback that steady state error of the system cannot be made absolutely zero. The controller gains need to be properly tuned to achieve satisfactory performance, which is generally achieved by using different optimization techniques [3]. A PID controller can also be used in place of a PI controller [4] but incorporation of a derivative term in the controller increases noise which might lead to system instability. Moreover, PI controller suffers from windup phenomenon where the integral term accumulates a large error which is compensated only with an offset by errors in the opposite direction. Thus, problems in overshoot and settling time are inherently associated with PID controllers. To mitigate the windup phenomenon in simple PID controller, anti-windup PI

controller has also been used in speed control of DC motor [5]. The PI based speed control loop can be augmented by adding a current control loop using a hysteresis controller. The hysteresis controller helps to limit the motor starting current while also reducing voltage and torque ripples [6]. This control technique, though simple, is however characterized by slow rise time as well as large settling time and appreciable peak overshoot.

To address the drawbacks of simple PI control, alternative approaches like deadbeat control, model predictive control (MPC) and fuzzy logic control were introduced [7-12]. MPC-based methods use system models and suitable cost function to predict and select a switching pattern. This brings down the complexity of the control algorithm but require extremely high sampling rate, which increases the cost of sensors and controllers. The performance improvement in case of fuzzy logic controllers is achieved at the cost of increased complexity in the controller design. A non-conventional method of speed control of DC motor using Artificial Neural Network (ANN) has been investigated in [13] where the neural network was trained to identify the inverse model of the motor without prior knowledge the motor's model. This approach however requires the neural network to be trained either online or offline using data sets to achieve desired performance. State feedback control is a modern control approach that aims to achieve control action by feeding back the state variables of the system. Since a very minimal number of state variables are involved in the speed control of a dc motor, the state feedback control approach is a lucrative one as it has been proven to achieve better control action compared to classical control approaches[14-15].

In state feedback control, the closed loop poles of the system are positioned at predefined points according to the desired closed loop response of the system in order to acquire the state feedback gains. The optimal control approach of state feedback is Linear Quadratic Regulator (LQR) control in which the closed loop poles of the system are obtained by optimizing a cost function based on the relative weights assigned to the state variables and the control variables. LQR is generally used to control a regulator system where the system input is zero while the controller forces the output state of the system to zero or an equilibrium state in the presence of external disturbances. So, to achieve speed control of dc motor, the reference tracking problem of the system needs to be converted into a regulator problem to implement LQR control. The existing research in the speed control of dc motor using LQR control approach is mostly focused on the output and response of the designed LQR controller with little emphasis on its modelling and design. Moreover, there is no

detailed mathematical derivation for implementing the LQR controller for a reference tracking problem in any existing research [16-19].

To address the aforementioned problems, a dc motor speed controller based on LQR control approach is designed in this paper and the performance of the controller is compared to that of the PI controller. The paper provides the mathematical formulation for converting the reference tracking problem of the speed control of a dc motor into a regulator problem in order to implement LQR control. The dc motor is modelled in MATLAB Simulink and a model verification is performed based on the parameters derived from an actual dc motor. LQR control is applied on this dc motor model to investigate the performance of the controller in terms of speed tracking and transient response.

## II. DC MOTOR MODELLING

The chopper-controlled dc motor drive is shown in Fig. 1. The armature of a separately excited dc motor can be modelled as series combination of resistance ( $R_a$ ), inductance ( $L_a$ ) and a voltage source ( $E_b$ ) representing the back emf.

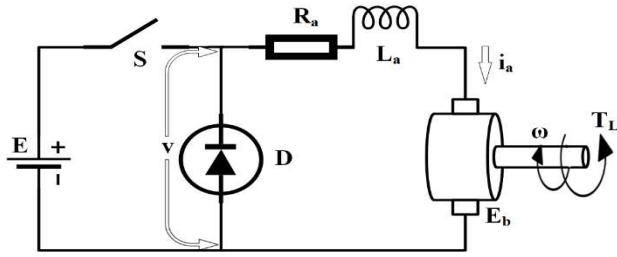


Fig. 1. Schematic for Chopper based DC Motor Drive

Writing the system equations based on Kirchhoff's laws:

$$V = \frac{L_a di_a}{dt} + i_a R_a + E_b \quad (1)$$

$$V = \frac{L_a di_a}{dt} + i_a R_a + K_e \omega \quad (2)$$

$$J_m \frac{d\omega}{dt} = K_m i_a - B_m \omega - T_L \quad (3)$$

where  $E_b = K_e \omega$ , the emf constant is  $K_e$ , the torque constant is  $K_m$ ,  $J_m$  is the total moment of inertia of the motor shaft,  $B_m$  is the viscous friction constant,  $\omega$  is the angular velocity of the motor and  $i_a$  is the armature current. The motor parameters are tabulated in Table I.

TABLE I. DC MOTOR PARAMETERS

Parameters	Values
$R_a$	12 $\Omega$
$L_a$	0.13 H
$K_e$	1.113 V/rad/s
$K_m$	1.14 Nm/A
$J_m$	0.004 kgm <sup>2</sup>
$B_m$	0.01 Nms

### A. Transfer Function Modelling

Transforming the time domain equations of the dc motor to frequency domain by taking the Laplace transformation, we obtain:

$$V(s) = sL_a I_a(s) + I_a(s)R_a + K_e \omega(s) \quad (4)$$

$$sJ_m \omega(s) = K_m I_a(s) - B_m \omega(s) - T_L(s) \quad (5)$$

Ignoring the load torque  $T_L$ , the open loop transfer function modelling the dc motor is obtained from equations (4-5) as:

$$G(s) = \frac{\omega(s)}{V(s)} = \frac{K_m}{J_m L_a s^2 + (B_m L_a + J_m R_a)s + K_m K_e} \quad (6)$$

Substituting the motor parameters from Table I in the above transfer function, we get:

$$G(s) = \frac{\omega(s)}{V(s)} = \frac{2192.31}{s^2 + 94.81s + 2671} \quad (7)$$

The block diagram of the open loop transfer function structure is shown in Fig. 2.

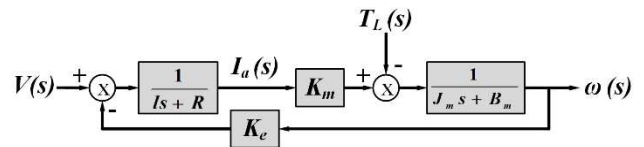


Fig. 2. Open Loop Transfer Function Block Diagram

### B. State Space Modelling

Taking  $i_a$  and  $\omega$  as the state vectors from equations (2-3), the of DC motor's state space representation can be expressed as:

$$\dot{X} = AX + BU \quad (8)$$

$$Y = CX \quad (9)$$

$$\begin{bmatrix} \dot{x}_1 \\ \dot{x}_2 \end{bmatrix} = \begin{bmatrix} \dot{\omega} \\ \dot{i}_a \end{bmatrix} = \begin{bmatrix} \frac{-B_m}{J_m} & \frac{K_m}{J_m} \\ \frac{-K_e}{L_a} & \frac{-R_a}{L_a} \end{bmatrix} \begin{bmatrix} \omega \\ i_a \end{bmatrix} + \begin{bmatrix} 0 \\ \frac{1}{L_a} \end{bmatrix} V \quad (10)$$

$$[y] = [\omega] = [1 \ 0] \begin{bmatrix} \omega \\ i_a \end{bmatrix}^T \quad (11)$$

Substituting the motor parameters from Table I in the state space equations, we get the system matrix A and input matrix B as:

$$A = \begin{bmatrix} -2.5 & 285 \\ -8.562 & -92.307 \end{bmatrix} \quad B = \begin{bmatrix} 0 \\ 7.69 \end{bmatrix} \quad C = [1 \ 0]$$

### C. Controllability, Observability and Stability Analysis

It is essential to analyse the controllability and observability of the existing motor dynamic system before building the controller for the motor speed tracking system. By determining if the controllability matrix is full rank, the controllability may be determined. The system's controllability discriminant matrix M is:

$$M = [B:AB] = \begin{bmatrix} 0 & \frac{K_m}{J_m L_a} \\ \frac{1}{L_a} & \frac{-R_a}{L_a^2} \end{bmatrix} \quad (12)$$

The controllability discriminant matrix M is full rank since  $K_m$  is non-zero, so the system is controllable. The observability is ascertained by judging whether the observability matrix is full

rank. The observability discriminant matrix  $N$  of the system is:

$$N = \begin{bmatrix} C \\ \cdots \\ CA \end{bmatrix} = \begin{bmatrix} 1 & 0 \\ -B_m & K_m \\ J_m & J_m \end{bmatrix} \quad (13)$$

The observability discriminant matrix  $N$  is full rank since  $K_m$  is non-zero, so the system is observable.

The eigen values of system matrix  $A$  govern the system's stability. The eigen values are obtained as:

$$|\lambda I - A| = 0 \quad (14)$$

$$\lambda_1 = -47.4035 + 20.5875i \quad (15)$$

$$\lambda_2 = -47.4035 - 20.5875i \quad (16)$$

Given that the real parts of the eigen values are negative and located on the left side of the  $s$ -plane, the system is stable.

### III. CONTROLLER DESIGN

#### A. Proportional Integral (PI) Controller

As the name suggests, PI controller consists of a proportional term ( $K_p$ ) and an integral term ( $K_i$ ). The  $K_p$  part decreases the rise time while the  $K_i$  part reduces the steady state error. Since the PI controller works satisfactorily with dc quantities, it is ideal as a motor speed controller. The transfer function of the PI controller is given by:

$$G_{PI}(s) = K_p + \frac{K_i}{s} \quad (17)$$

Fig. 3 depicts the closed loop system using the PI controller, and its overall transfer function is provided by:

$$H(s) = \frac{(K_i + K_p s)K_m}{J_m L_a s^3 + (B_m L_a + J_m R_a) s^2 + K_m K_e s} \quad (18)$$

The controller was tuned with  $K_p = 7$  and  $K_i = 200$  using bandwidth approach [20] to achieve satisfactory result. Substituting the values of  $K_p$ ,  $K_i$  and motor parameters from Table I in the above transfer function, we get:

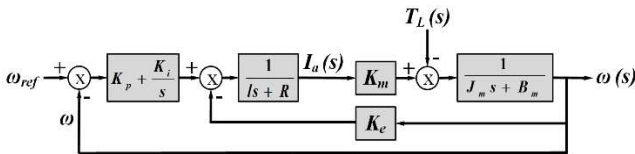


Fig. 3. Closed Loop Transfer Function Block Diagram

$$H(s) = \frac{98653.846s + 219.23}{s^3 + 94.81s^2 + 2440.04s} \quad (19)$$

#### B. Linear Quadratic Regulator (LQR) Controller

As the name suggests, the LQR controller is generally used for a regulator system, i.e. when the external input to the system is zero. However, for the purpose of reference speed tracking in the case of dc motor speed control, the reference tracking problem needs to be modified into a regulator problem for implementing LQR.

For the dc motor system described by equations (8-11), the closed loop control system with state feedback and error comparator is shown in Fig. 4.

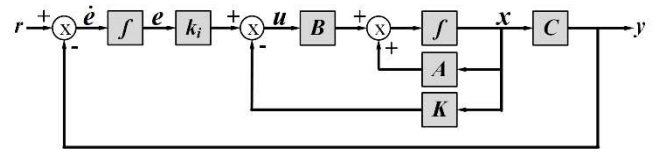


Fig. 4. Closed Loop State Space Block Diagram

From the diagram we obtain:

$$u = -KX + k_i e \quad (20)$$

$$\dot{e} = r - Y = r - CX \quad (21)$$

Where  $r$  is the reference speed signal,  $e$  is the output of the error integrator and  $k_i$  is the integral gain of the error integrator.

For  $t > 0$ , the system dynamics can be described by a combination of equations (8), (9) and (21).

$$\begin{bmatrix} \dot{X}(t) \\ \dot{e}(t) \end{bmatrix} = \begin{bmatrix} A & 0 \\ -C & 0 \end{bmatrix} \begin{bmatrix} X(t) \\ e(t) \end{bmatrix} + \begin{bmatrix} B \\ 0 \end{bmatrix} u(t) + \begin{bmatrix} 0 \\ 1 \end{bmatrix} r(t) \quad (22)$$

An asymptotically stable system can be designed such that  $x(\infty)$ ,  $e(\infty)$ , and  $u(\infty)$  approach constant values, respectively. Then, at steady state we get,  $\dot{e}(t) = 0$  and  $y(\infty) = r$ . So, Equation (22) at steady state becomes:

$$\begin{bmatrix} \dot{X}(\infty) \\ \dot{e}(\infty) \end{bmatrix} = \begin{bmatrix} A & 0 \\ -C & 0 \end{bmatrix} \begin{bmatrix} X(\infty) \\ e(\infty) \end{bmatrix} + \begin{bmatrix} B \\ 0 \end{bmatrix} u(\infty) + \begin{bmatrix} 0 \\ 1 \end{bmatrix} r(\infty) \quad (23)$$

$r(t)$  being a step input, we get  $r(\infty) = r(t) = r$  (constant) for  $t > 0$ . By subtracting equation (23) from Equation (22), we get:

$$\begin{bmatrix} \dot{X}(t) - \dot{X}(\infty) \\ \dot{e}(t) - \dot{e}(\infty) \end{bmatrix} = \begin{bmatrix} A & 0 \\ -C & 0 \end{bmatrix} \begin{bmatrix} X(t) - X(\infty) \\ e(t) - e(\infty) \end{bmatrix} + \begin{bmatrix} B \\ 0 \end{bmatrix} [u(t) - u(\infty)] \quad (24)$$

Defining a new set of variables as:

$$X(t) - X(\infty) = X_e(t) \quad (25)$$

$$e(t) - e(\infty) = e_e(t) \quad (25)$$

$$u(t) - u(\infty) = u_e(t)$$

Equation (27) can now be re-written as:

$$\begin{bmatrix} \dot{X}_e(t) \\ \dot{e}_e(t) \end{bmatrix} = \begin{bmatrix} A & 0 \\ -C & 0 \end{bmatrix} \begin{bmatrix} X_e(t) \\ e_e(t) \end{bmatrix} + \begin{bmatrix} B \\ 0 \end{bmatrix} u_e(t) \quad (26)$$

Where,

$$u_e(t) = -(KX_e(t) - k_i e_e(t)) = -\hat{K} \begin{bmatrix} X_e(t) \\ e_e(t) \end{bmatrix} \quad (27)$$

such that

$$\hat{K} = [k_1 \quad k_2 \quad -k_i] \quad (28)$$

Defining a new  $(n+1)^{\text{th}}$  order error vector  $E(t)$  by:

$$E(t) = \begin{bmatrix} X_e(t) \\ e_e(t) \end{bmatrix} \quad (29)$$

Equation (29) becomes:

$$\dot{E} = \hat{A}E + \hat{B}u_e \quad (30)$$

$$\text{where } \hat{A} = \begin{bmatrix} A & 0 \\ -C & 0 \end{bmatrix} \text{ and } \hat{B} = \begin{bmatrix} B \\ 0 \end{bmatrix}$$

Before obtaining the values of  $k$  using LQR, the controllability of the modified system needs to be checked. If the matrix  $M$  has rank  $(n+1)$ , where  $n$  is the system's order, then the modified system is fully state controllable. [21].

$$M = \begin{bmatrix} A & B \\ -C & 0 \end{bmatrix} = \begin{bmatrix} -B_m/J_m & K_m/J_m & 0 \\ -K_e/L_a & -R_a/L_a & 1/L_a \\ -1 & 0 & 0 \end{bmatrix} \quad (31)$$

Substituting the motor parameters in equation (31), the rank of the controllability matrix is obtained to be 3. So, the system is completely state controllable. Now the response of the system can be obtained by solving the following equation obtained by substituting equation (27) in (26).

$$\begin{bmatrix} \dot{X} \\ \dot{e} \end{bmatrix} = \begin{bmatrix} A-BK & Bk_i \\ -C & 0 \end{bmatrix} \begin{bmatrix} X \\ e \end{bmatrix} + \begin{bmatrix} 0 \\ 1 \end{bmatrix} r \quad (32)$$

$$Y = [1 \ 0 \ 0] \begin{bmatrix} X \\ e \end{bmatrix} \quad (33)$$

For an LTI system with the above state equations, the solution of the LQR problem pertains to minimizing the cost function  $J$ :

$$J = \frac{1}{2} \int_0^{\infty} (X^T Q X + U^T R U) dt \quad (34)$$

The optimal problem solution involves finding the optimal control input  $U$  which minimizes the energy of the final state, all intermediate states and also that of the control used to achieve this. Minimizing the energy refers to keeping both the state and control close to zero or to be driven back to their equilibrium state. The faster this is achieved, the better is the system performance and lower is the cost. Here  $Q$  and  $R$  are symmetric positive semi-definite matrices. If it is necessary to make the intermediate states small, then the values of the elements of the  $Q$  matrix should be chosen to be large to weight it heavily in  $J$ . If the control energy is required to be small, then the values of the elements of the  $R$  matrix should be chosen to be large to weight it heavily in  $J$ . Thus,  $Q$  is called state weighting matrix and  $R$  is called the control weighting matrix. The optimal control is achieved by finding the solution  $S$  of the Algebraic Riccati Equation (ARE):

$$SA + A^T S - SBR^{-1}B^T S + Q = 0 \quad (35)$$

The optimal control input  $U$  is given by:

$$U = -R^{-1}B^T S X \quad (36)$$

The feedback gain matrix  $K$  is given by:

$$K = -R^{-1}B^T S \quad (37)$$

The value for  $K$  is obtained from MATLAB by using the function `lqr(A, B, Q, R)` as  $k_1 = 0.9763$ ,  $k_2 = 2.712$  and  $k_i = 31.6228$ .

As previously mentioned, larger value of  $Q$  means the system reaches stability with less change in the states while

smaller value of  $Q$  means that the states would have larger variation.

Similarly, with larger value of  $R$ , the system reaches stability with lesser control input signals whereas more energy is required with smaller value of  $R$ . For the designed system, higher value of  $Q$  is chosen for  $q_{33}$  to stabilize the speed error tracking. The value of  $Q$  and  $R$  are chosen as:

$$Q = \begin{bmatrix} 0.1 & 0 & 0 \\ 0 & 0.1 & 0 \\ 0 & 0 & 1000 \end{bmatrix} \quad R = 1.75$$

#### IV. SIMULATION AND RESULTS

The dc motor was simulated in MATLAB Simulink with parameters obtained from an actual dc motor and the step response of the system was observed for open loop system, PI controlled system and LQR controlled system. It is seen from Fig. 5 that the open loop system is unable to reach steady state value and settles to a final value of 0.8. With the incorporation of the PI controller, the closed loop system is able to attain the steady state value but with a maximum peak overshoot of nearly 40%. The closed loop system with LQR control achieves the steady state value with no overshoot. But the rise time and settling time has a higher value than that of the open loop system and PI controlled system. The transient characteristics of the step responses for open loop, PI controlled and LQR controlled system are shown in Table II.

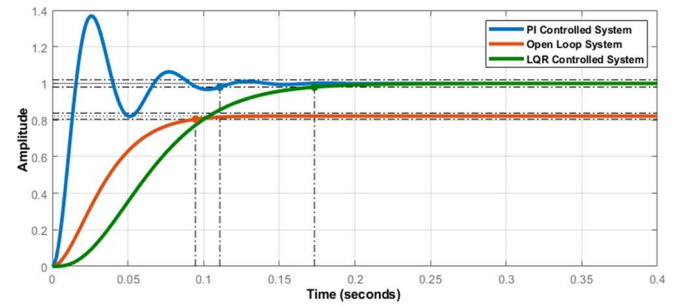


Fig. 5. Step response of open loop system, PI controlled system and LQR controlled system .

TABLE II. TRANSIENT CHARACTERISTICS

Parameters	Open Loop	PI Controller	LQR Controller
Rise Time ( $t_r$ )	0.0573s	0.0105s	0.0965s
Settling Time ( $t_s$ )	0.0946s	0.111s	0.173s
Peak Overshoot ( $M_p$ )	0%	36.9%	0%

Next the error tracking performance of the PI controller and the LQR controller is examined by providing step reference inputs for the dc motor speed. It is observed from Fig. 6(a) and Fig. 6(d) that the PI controller is able to track the reference speed with an initial overshoot but the LQR controller has no overshoot and the system tracks the reference speed smoothly. The overshoot problem of PI controller is due to the windup phenomenon as initially discussed. The smooth speed tracking of the LQR controller is attributed to the high value of state weighing matrix  $Q$  corresponding to the speed error tracking. In both the cases, the system is able to track the change in reference speed from 1000 rpm to 1500 rpm.

The armature voltage waveform for the PI controlled system has initial oscillations during motor start and also during speed change as shown in Fig. 6(b). However, the arm-

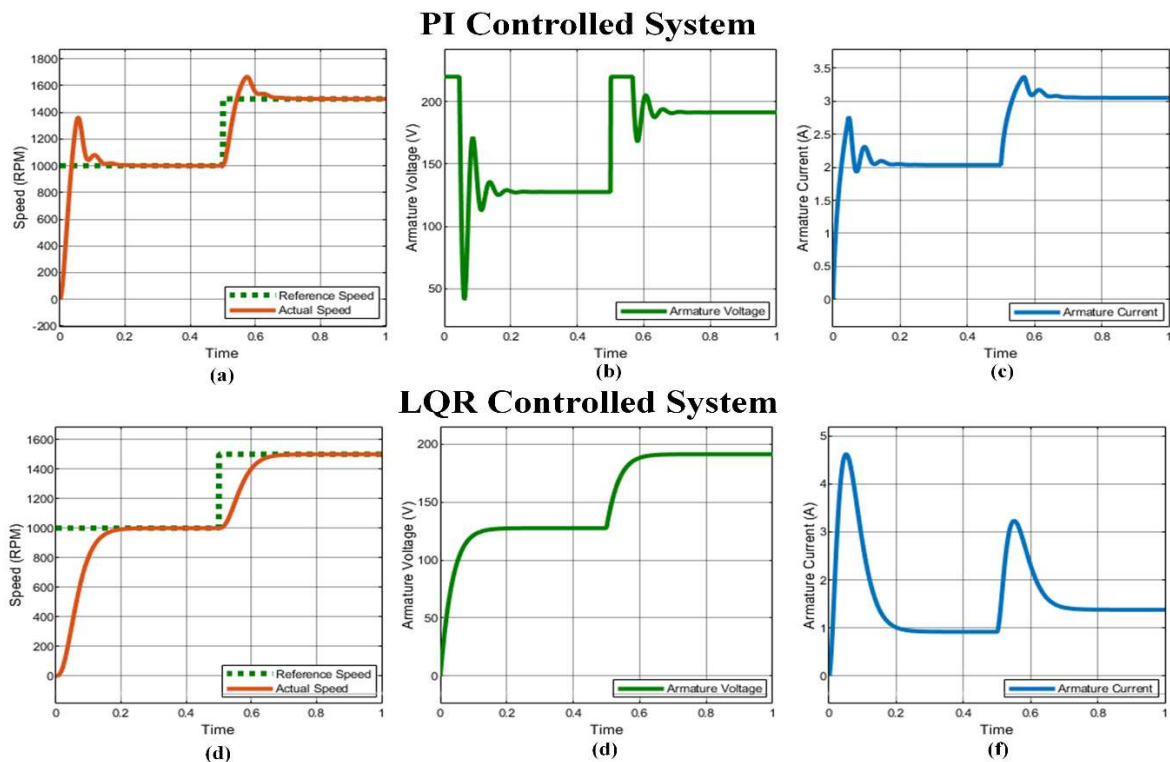


Fig. 6. (a) Speed tracking of PI controlled system (b) Armature Voltage of PI controlled system (c) Armature Current of PI controlled system (d) Speed tracking of LQR controlled system (e) Armature Voltage of LQR controlled system (f) Armature Current of LQR controlled system

ature voltage profile for the LQR controlled system is smooth without any oscillations during the entire startup and speed change process as shown in Fig. 6(e).

Fig. 6(c) shows that the PI controlled system draws 2A current during the initial speed of 1000 rpm and 3A current during the final speed of 1500 rpm. The LQR controlled system draws 1A current during the initial speed and 1.5A current during the final speed as shown in Fig. 6(f). Thus, the overall armature current is reduced to half with LQR control. However, it is seen that the initial starting current is higher with LQR control than with PI control, which is attributed to the fact that the value for state weighting matrix  $Q$  corresponding to current tracking has been chosen to be small.

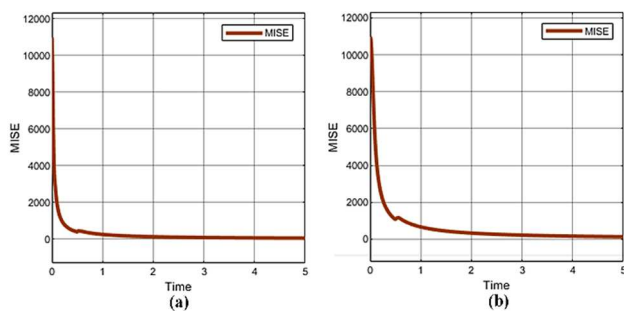


Fig. 7. (a) MISE of PI controlled system (b) MISE of LQR controlled system

The mean integral square error (MISE) curves of Fig. 7(a) and Fig. 7(b) shows that the error is reduced to zero for both the PI controlled and LQR controlled system, thereby ensuring satisfactory speed tracking of the DC motor.

## V. CONCLUSION

This paper presents the speed control technique of a DC motor using LQR control and provides a mathematical

background to implement such a control strategy in respect to a reference tracking problem. The performance of the designed controller is compared to that of a classical PI controller in terms of transient response and reference tracking capability. The armature voltage and armature current profiles for both PI controlled and LQR controlled system are also analysed. It is seen that both the PI controller and the LQR controller are able to achieve steady state reference speed value. The PI controlled system exhibits a fast rise time and settling time but with a considerable peak overshoot. On the other hand, the LQR controlled system has no overshoot but slightly higher rise time and settling time compared to the PI controller. The armature voltage profile for the PI controlled system has oscillations during initial start-up and speed change which are smoothened out in case of the LQR controlled system. The overall armature current is also reduced for a LQR controller as compared to a PI controller. The slightly higher rise time and settling time of the LQR controller is attributed to the fact that LQR control does not provide the best solution but provides an optimal solution to the problem by achieving a trade-off between rise time, settling time and maximum peak overshoot based on the values of the chosen state and control weighting matrices. The future scope of this work would be to include a hardware implementation to ascertain the validity of the simulations and also study the impact of external disturbances like variation of load torque on the performance of the designed LQR controller. Further, a comparison can be made on the performance of the LQR controller with variations in  $Q$  and  $R$  matrices.

## REFERENCES

- [1] M. A. Ibrahim, A. N. Hamoodi, and B. M. Salih, "PI controller for DC motor speed realized with simulink and practical measurements," *Int. J. Power Electron. Drive Syst.*, vol. 11, no. 1, pp. 119–126, 2020, doi: 10.11591/ijpeds.v11.i1.pp119-126.



- [2] H. Maghfiroh, A. Ataka, O. Wahyunggoro, and A. I. Cahyadi, "Optimal energy control of DC Motor speed control: Comparative study," *Proceeding - 2013 Int. Conf. Comput. Control. Informatics Its Appl. "Recent Challenges Comput. Control Informatics"*, IC3INA 2013, pp. 89–93, 2013, doi: 10.1109/IC3INA.2013.6819154.
- [3] V. Vishal, V. Kumar, K.P.S. Rana and P. Mishra, "Comparative Study of Some Optimization Techniques Applied to DC Motor Control," 2014 IEEE International Advance Computing Conference (IACC), pp. 1342–1347, 2014, doi: 10.1109/IAdCC.2014.6779522.
- [4] C. Agarwal and A. Gupta, "Modeling, simulation based DC motor speed control by implementing PID Controller on FPGA," *IET Conf. Publ.*, vol. 2013, no. 647 CP, pp. 467–471, 2013, doi: 10.1049/cp.2013.2358.
- [5] M. Tariq, T. K. Bhattacharya, N. Varshney, and D. Rajapan, "Fast response Antiwindup PI speed controller of Brushless DC motor drive: Modeling, simulation and implementation on DSP," *J. Electr. Syst. Inf. Technol.*, vol. 3, no. 1, pp. 1–13, 2016, doi: 10.1016/j.jesit.2015.11.008.
- [6] A. P. C. Rao, Y. P. and C. H. Sai, "Performance Improvement of BLDC Motor with Hysteresis Current Controller," *Int. J. Adv. Res. Electr. Electron. Instrum. Energy*, pp. 5900–5907, 1970.
- [7] J. Jing, Y. Wang, and Y. Huang, "The Fuzzy-PID Control of Brushless DC Motor," no. 2, pp. 1440–1444, 2016.
- [8] D. Gu, J. Zhang, and J. Gu, "Brushless DC motor speed control based on predictive functional control," *Proc. 2015 27th Chinese Control Decis. Conf. CCDC 2015*, no. 4, pp. 3456–3458, 2015, doi: 10.1109/CCDC.2015.7162520.
- [9] S. Sahoo and B. Subudhi, "Quadratic Regulator and Model Predictive Control," 2015 Int. Conf. Energy, Power Environ. Towar. Sustain. Growth, no. 2, pp. 1–5, 2015.
- [10] M. Dursun and S. Engin, "Deadbeat control of a DC servo motor at low speed," *Proc. - 2018 4th Int. Conf. Control. Autom. Robot. ICCAR 2018*, pp. 282–286, 2018, doi: 10.1109/ICCAR.2018.8384685.
- [11] S. N. Thanh, C. N. The, and H. H. Xuan, "Improved performance of a sensorless DC motor control using fuzzy logic," 2014 5th Int. Conf. Intell. Adv. Syst. Technol. Conver. Sustain. Futur. ICIAS 2014 - Proc., 2014, doi: 10.1109/ICIAS.2014.6869506.
- [12] L. Ardhenta and R. K. Subroto, "Feedback Control for Buck Converter - DC Motor Using Observer," 2020 12th Int. Conf. Electr. Eng. ICEENG 2020, pp. 30–33, 2020, doi: 10.1109/ICEENG45378.2020.9171693.
- [13] E. Buzi and P. Marango, "A comparison of conventional and nonconventional methods of DC motor speed control," vol. 15, no. PART 1. IFAC, 2013, doi: 10.3182/20130606-3-XK-4037.00054.
- [14] A. Maarif and N. R. Setiawan, "Control of dc motor using integral state feedback and comparison with pid: Simulation and arduino implementation," *J. Robot. Control*, vol. 2, no. 5, pp. 456–461, 2021, doi: 10.18196/jrc.25122.
- [15] R. M. T. Raja Ismail, M. A. Ahmad, and M. S. Ramli, "Speed control of buck-converter driven dc motor using LQR and PI: A comparative assessment," *Proc. - 2009 Int. Conf. Inf. Manag. Eng. ICIME 2009*, pp. 651–655, 2009, doi: 10.1109/ICIME.2009.8.
- [16] V. Saisudha, G. Seeja, R. V. Pillay, G. Manikutty, and R. R. Bhavani, "Analysis of speed control of DC motor using LQR method," *Int. J. Control Theory Appl.*, vol. 9, no. 15, pp. 7377–7385, 2016.
- [17] R. Dwivedi and D. Dohare, "PID Conventional Controller and LQR Optimal controller for Speed analysis of DC Motor: A Comparative Study," *Int. Res. J. Eng. Technol.*, pp. 508–511, 2015.
- [18] T. T. Nguyen, "The linear quadratic regular algorithm-based control system of the direct current motor," *Int. J. Power Electron. Drive Syst.*, vol. 10, no. 2, pp. 768–776, 2019, doi: 10.11591/ijpeds.v10.i2.pp768-776.
- [19] S. Dani, D. Sonawane, D. Ingole, and S. Patil, "Performance evaluation of PID, LQR and MPC for DC motor speed control," 2017 2nd Int. Conf. Conver. Technol. I2CT 2017, vol. 2017-Janua, pp. 348–354, 2017, doi: 10.1109/I2CT.2017.8226149.
- [20] E. B. and V. C. Janeth Alcalá, "Practical Methods for Tuning PI Controllers in the DC-Link Voltage Loop in Back-to-Back Power Converters," in 12th IEEE International Power Electronics Congress, 2010, pp. 46–52, doi: 10.1109/CIEP.2010.5598898.
- [21] K. Ogata, *Modern Control Engineering [Paperback]*. 2009.